HHS Public Access

Author manuscript

Oncogene. Author manuscript; available in PMC 2019 August 12.

Published in final edited form as:

Oncogene. 2018 December ; 37(50): 6463–6476. doi:10.1038/s41388-018-0424-8.

RANBP9 affects cancer cells response to genotoxic stress and its overexpression is associated with worse response to platinum in NSCLC patients

Anna Tessari[1], **Kareesma Parbhoo**[1], **Meghan Pawlikowski**[1], **Matteo Fassan**[2], **Eliana Rulli**[3], **Claudia Foray**[1], **Alessandra Fabbri**[4], **Valerio Embrione**[1], **Monica Ganzinelli**[5], **Marina Capece**[1], **Moray J. Campbell**[6], **Massimo Broggini**[3], **Krista La Perle**[7], **Gabriella Farina**[8], **Sara Cole**[9], **Mirko Marabese**[3], **Marianna Hernandez**[1], **Joseph M. Amann**[10], **Giancarlo Pruneri**[11], **David P. Carbone**[10], **Marina C. Garassino**[5], **Carlo M. Croce**[1], **Dario Palmieri**[1], **Vincenzo Coppola**[1]

[1]Department of Cancer Biology and Genetics, College of Medicine, The Ohio State University and Arthur G. James Comprehensive Cancer Center, Columbus, OH 43210, USA

[2]Department of Medicine (DIMED), Surgical Pathology Unit, University of Padua, Padua, Italy

[3]Department of Oncology, IRCCS - Istituto di Ricerche Farmacologiche Mario Negri, Milan, Italy

[4]Department of Pathology and Laboratory Medicine, Fondazione IRCCS Istituto Nazionale dei Tumori, Milan, Italy

[5]Thoracic Oncology Unit, Department of Medical Oncology, Fondazione IRCCS, Istituto Nazionale dei Tumori, Milan, Italy

[6]Division of Pharmaceutics and Pharmaceutical Chemistry, College of Pharmacy, The Ohio State University, 536 Parks Hall, Columbus, OH 43210, USA

[7]Department of Veterinary Biosciences and Comparative Pathology and Mouse Phenotyping Shared Resource, College of Veterinary Medicine, The Ohio State University and Arthur G. James Comprehensive Cancer Center, Columbus, OH, USA

[8]Department of Oncology, Ospedale Fatebenefratelli and Oftalmico, Milan, Italy

[9]Campus Microscopy and Imaging Facility, The Ohio State University, Columbus, OH 43210, USA

[10]Department of Internal Medicine, College of Medicine, James Thoracic Center, Ohio State University and Arthur G. James Comprehensive Cancer Center, Columbus, OH 43210, USA

[11]Division of Pathology, Fondazione IRCCS, Istituto Nazionale dei Tumori, Milan, Italy

Abstract

Although limited by severe side effects and development of resistance, platinum-based therapies still represent the most common first-line treatment for non-small cell lung cancer (NSCLC). However, a crucial need in the clinical management of NSCLC is represented by the identification

Vincenzo Coppola vincenzo.coppola@osumc.edu.

Conflict of interest The authors declare that they have no conflict of interest.

of cases sensitive to DNA damage response (DDR)-targeting drugs, such as cisplatin or PARP inhibitors. Here, we provide a molecular rationale for the stratification of NSCLC patients potentially benefitting from platinum compounds based on the expression levels of RANBP9, a recently identified player of the cellular DDR. RANBP9 was found overexpressed by immunohistochemistry (IHC) in NSCLC compared to normal adjacent tissues (NATs) (n = 147). Moreover, a retrospective analysis of 132 platinum-treated patients from the multi-centric TAILOR trial showed that RANBP9 overexpression levels are associated with clinical response to platinum compounds [Progression Free Survival Hazard Ratio $_{(\text{RANBP9 high vs low})}$ 1.73, 95% CI 1.15–2.59, p = 0.0084; Overall Survival HR $_{(\text{RANBP9 high vs low})}$ 1.99, 95% CI 1.27–3.11, p = 0.003]. Accordingly, RANBP9 KO cells showed higher sensitivity to cisplatin in comparison with WT controls both in vitro and in vivo models. NSCLC RANBP9 KO cells were also more sensitive than control cells to the PARP inhibitor olaparib alone and in combination with cisplatin, due to defective ATM-dependent and hyper-activated PARP-dependent DDR. The current investigation paves the way to prospective studies to assess the clinical value of RANBP9 protein levels as prognostic and predictive biomarker of response to DDR-targeting drugs, leading to the development of new tools for the management of NSCLC patients.

Introduction

Lung cancer (LC) is the leading cause of cancer deaths in the world [1] and includes two main groups: Non-Small Cell Lung Cancers (NSCLC, ~85% of the cases) and small-cell lung cancers (~15% of total LC). NSCLC is further divided in subgroups of which Adenocarcinoma (LUAD, ~40%) and Squamous Cell Lung Cancer (LUSC, ~25–30%) are the most frequent (www.cancer.org/cancer/non-small-cell-lung-cancer/about/key-statistics.html). Unfortunately, only 16% of patients display localized disease at diagnosis, while a vast majority present regional (22%) or distant (57%) tumor spread. Five-year survival rates range from 67% for patients with T1N0 disease, to 23% for T1–3N2 disease, to about 1–10% for metastatic patients [2]. Despite the development of targeted therapies [3, 4] and the use of immune-checkpoint inhibitors [5], over 50% of NSCLC patients still do not benefit from those drugs [6]. Current first-line treatment for NSCLC mostly employs platinum-based chemotherapy [7], but a growing body of evidence indicates that combination therapies including chemotherapy and immune-checkpoint inhibitors (anti-PD-1/PD-L1 antibodies) might result in better treatment outcomes [8, 9]. Cis-diamminedichloroplatinum(II) (Cisplatin, CDDP), and its analogues oxaliplatin and carboplatin, cause various types of DNA crosslinks, single and double strand breaks (DSBs) [7, 10, 11], leading to cell cycle arrest and, eventually, cell death. Although a significant number of patients initially respond favorably to platinum-based regimens, the majority of them display severe side effects and de novo or acquired resistance to platinum compounds [12–16]. Thus, predictive biomarkers and new combination therapies represent a major unmet clinical need [17].

RANBP9 (a.k.a. RAN Binding Protein Microtubule organizing center, RANBPM) is a ubiquitous, evolutionarly conserved scaffold protein present both in the cell nucleus and cytoplasm, whose functions are still poorly characterized [18, 19].

We have recently demonstrated that RANBP9 is both a target and a signaling facilitator of the Ataxia Telangiectasia Mutated (ATM) protein, the pinnacle kinase of the cellular DNA damage response (DDR) [20]. In NSCLC cells, RANBP9 rapidly accumulates in the nucleus in an ATM phosphorylation-dependent manner following exposure to ionizing radiation [20]. RANBP9 silencing results in reduced activation of the ATM pathway, deficiency of the homology-directed repair (HDR), and enhanced sensitivity to genotoxic treatments [20]. Accordingly, RANBP9 emerged as one of the top genes linked to sensitivity to DNA damage from a high-throughput screening of 522 cell lines [21].

Here, we evaluated the clinical relevance of RANBP9 expression in human lung tumors and assessed its potential use in diagnosis and treatment of LC patients. We also performed in vitro and in vivo experiments showing increased sensitivity to platinum compounds and PARP inhibitors of NSCLC cells in which RANBP9 is genetically ablated.

Materials and methods

Patients, tissues, tissue micro arrays (TMAs) and immunohistochemical analysis

For the evaluation of RANBP9 expression in normal lung tissues and in biopsies from lung cancer patients, OD-CT-RsLug01–007, OD-CT-RsLug01–009, and BC04022a Tissue MicroArrays were purchased from US Biomax (US Biomax Inc). OD-CT-RsLug01–007 is composed by 60 tumor samples and the associated normal adjacent tissue (NAT), equally divided in six different lung cancer subtypes: adenocarcinoma, squamous carcinoma, adenosquamous carcinoma, bronchioalveolar carcinoma, large cell carcinoma, small cell lung cancer. Among the squamous cell carcinoma and small cell lung cancer samples, nine out of ten samples were evaluable. OD-CT-RsLug01–009 is composed by 75 cases of lung squamous cell carcinoma and matched NAT. A total of 71 samples were evaluable. BC04022a is composed by 18 cases of lung squamous cell carcinoma and matched NAT. Eighteen cases were evaluable. For the evaluation of RANBP9 expression, an H-score > 10 was considered as positive. Statistical significance was analyzed according to two-tailed Fisher exact test.

For the evaluation of RANBP9 expression in primary lung tumors and nodal metastases, 30 FFPE primary lung adenocarcinomas and their relative synchronous lymph node metastasis were analyzed (M/F = 18/12; age 70.2 ± 10.4). Patients were obtained from the University of Padua, and the study was approved by the local ethic Committee (n. 1721/16). All the samples were processed using the Galileo CK3500 Arrayer (www.isenet.it), a semiautomatic and computer-assisted tissue macro array (TMA) platform. Two 1-mm cores were obtained from both the primary and the metastatic lesions and included in three TMAs. Automated immunohistochemical (IHC) staining was performed using the Bond Polymer Refine Detection kit (Leica Biosystems, Newcastle upon Tyne, UK) in the BOND-MAX system (Leica Biosystems) on 4 μm-thick FFPE sections with the primary antibodies for RANBP9 (HPA050007; Sigma-Aldrich, Saint Louis, MI). For the evaluation of RANBP9 expression, an H-score > 10 was considered as positive. The correlation between primary and nodal RANBP9 expression was calculated according to Pearson Correlation Coefficient (http://www.socscistatistics.com/tests/pearson/Default2.aspx).

For the evaluation of RANBP9 expression on NSCLC patients who had received platinum-based therapies as first-line treatment, TMAs from patients enrolled in the TAILOR trial were stained as described above. A comprehensive description of the clinical trial is reported elsewhere [22]. The study was approved by the Ethics Committee of Ospedale Fatebenefratelli e Oftalmico, Milan (03 October 2007) and was performed in accordance with the principles of the Declaration of Helsinki. All eligible patients provided written informed consent. Samples with either H-score > 100 or at least 10% of cells with moderate to strong RANBP9 intensity staining were considered as high-RANBP9.

Validation of commercially available anti-RANBP9 antibody (HPA050007) for IHC purpose (see below) was performed on 5 NSCLC tumors and matching NAT samples obtained from the Tissue Procurement Service of the Local University. Written informed consent was provided by patients after review and approval of a specified protocol by the University institutional review committee. Fresh frozen samples were used for protein and RNA extraction, as described below. Immunohistochemical staining was performed as above, with the only difference of the use of Nova Red for the staining from anti-RANBP9 antibody.

Validation of anti-RANBP9 antibody for IHC staining

We selected a commercially available anti-RANBP9 specific antibody (rabbit HPA-050007, Sigma), approved for IHC by the Human Protein Atlas project (http://www.proteinatlas.org/). Western Blot (WB) analysis using a different commercially available antibody (rabbit Abcam ab64275) confirmed RANBP9 positivity detected by IHC with the HPA-050007 antibody.

To further validate this antibody, we generated subcutaneous xenografts using previously described and validated H460 and H1299 lung cancer cells, stably transduced with an anti-RANBP9 shRNA (shRANBP9) or control vector (shCTRL) [20]. A total of 2×10^6 viable shCTRL- or shRANBP9-H460 and shCTRL- or shRANBP9-H1299 were injected subcutaneously into the left and right flank of 5-wk-old nude mice. At 3 weeks from injection, tumors were dissected and fixed in 10% formalin before paraffin embedding for IHC staining (Figure S2A). As shown in Figure S2B–C, in five different cases of NSCLC (3 LUAD, 2 LUSC) and in the paired NAT, the IHC staining for RANBP9 was consistent with the WB. Notably, we did not observe a direct correlation between RANBP9 protein (assessed by IHC and WB using two different antibodies, Figure S2B–C) and mRNA levels (evaluated by real-time PCR, Figure S2D).

In vivo studies

Animal experiments were performed according to University institutional guidelines after review by an institutional review board. Athymic, immune-compromised (nude) mice were obtained from a shared resource at the University, originally obtained from NCI/Charles River and maintained in an outbred breeding scheme. A total of 5×10^6 viable A549 *RANBP9* WT or *RANBP9* KO were injected subcutaneously into the left and right flank of 5-wk-old female nude mice. At 3 weeks from injection, tumor mass was measured using a caliper and mice with comparable tumor size were divided into groups including at least three animals. Mice were then treated with 5 mg/Kg of CDDP or with control buffer (0.9%

NaCl in water), once a week for 3 weeks, and treatment was then suspended for one week. Tumor size was measured twice per week until euthanasia, as described in the results. The experiment was not performed in blind. Tumor volume was calculated using the formula (long diameter × short diameter^2)/2. Tumors were dissected and fresh frozen before protein and RNA extraction, or fixed in 10% Formalin before paraffin embedding for IHC staining. Statistical significance was analyzed by unpaired Student *t*-test.

Statistical analysis

Statistical significance for quantitative experiments was analyzed by unpaired Student *t*-test. Results were considered significant for *p*-values < 0.05 (*$p < 0.05$; **$p < 0.01$; ***$p < 0.001$). Two-tailed Fisher exact test and Pearson correlation coefficient were used to assess the statistical significance of RANBP9 expression in IHC staining experiments, as described below.

Chi-square test and *t*-test were used to analyze associations between RANBP9 expression status and clinical characteristics. PFS was defined as the time from the first line treatment start to the date of progression or death from any cause, whichever came first. OS was defined as the time from the first line treatment start up to the date of death from any cause. Subjects who had not progressed or died while on study were censored at the last disease assessment date. Survival curves were estimated with the Kaplan–Meier method. Univariate and multivariate Cox proportional hazards models were used for univariate and multivariate (adjusted for ECOG-PS, sex, histotype, smoke, and treatment arm) analysis to analyze the impact of RANBP9 expression on PFS and OS. Results were expressed as Hazard Ratios (HRs) and their 95% confidence intervals (95% CIs). Subgroups analysis according to clinical stage was performed. All statistical tests were two-sided and a *p*-value < 0.05 was considered statistically significant. Statistical analyses were carried out using SAS version 9.4 (SAS Institute, Cary, NC).

Results

Lung tumors show high levels of RANBP9 protein

First, we analyzed RANBP9 protein levels by IHC in human LC tissues and paired NATs. To this aim, we used an antibody approved by the Human Protein Atlas (see ‘Materials and methods’). In the first Tissue MicroArray (TMA; OD-CT-RsLug01–007; $n = 58$) RANBP9 was significantly overexpressed in the nuclei of tumors versus NATs in all LC histotypes and in the cytoplasm of tumors vs NATs for adenocarcinoma (LUAD), Adenosquamous, Bronchioalveolar and Small-Cell Carcinoma ($p < 0.05$; Fig. 1a and Table S1). As shown in Table S2, RANBP9 was significantly overexpressed both at cytoplasmic and nuclear level ($p < 0.001$) also in two larger cohorts of lung squamous cell carcinomas (LUSC) compared to paired NATs (OD-CT-RsLug01–009 and BC04022a, $n = 89$). These results were in agreement with a bioinformatics analysis of the COSMIC and TCGA database (Figure S1A–B and Table S3).

In vitro, A549, H460, and H1299 NSCLC cell lines all showed increased amount of RANBP9 in comparison with normal-like bronchial epithelium cell lines BEAS-2B and

HBEC3-KT (Figure S1C). However, we did not observe a direct correlation between RANBP9 protein and mRNA levels neither in cancer cell lines (Figure S1D) nor in lung tumors (Figure S2).

Taken together, these results show that RANBP9 is frequently overexpressed in LC tumors and cell lines, but mRNA levels do not always positively correlate with protein levels.

Next, we analyzed by IHC primary tumor and the available nodal metastasis from a cohort of 30 LUAD patients, not part of the commercially available TMAs used above and obtained from the Department of Medicine (DIMED), Surgical Pathology Unit, University of Padua, Padua, Italy. Notably, nodal lesions frequently displayed similar or higher levels of RANBP9, in comparison to the respective primary tumors (Fig. 1b, c). Moreover, a positive correlation was found between RANBP9 expression levels in the primary tumor and in the associated nodal lesion.

These results demonstrate that RANBP9 overexpression is maintained or increased LC cells during the process of metastatization.

Ablation of RANBP9 increases sensitivity of NSCLC cells to cisplatin in vitro and in vivo

A549, H460, and H1299 cells stably silenced for RANBP9 show reduced ATM activation, defective HDR, and enhanced apoptosis following genotoxic stress [20]. Here, we aimed to emphasize the importance of RANBP9 in the cellular DDR by generating LC cell lines in which its expression was abrogated by CRISPR/Cas9 (Figure S3A–B). Although we obtained similar results with different cellular models of LC (Figure S3C–D), we mostly focused our study on A549 cells, one of the most common in vitro model of LUAD [23].

A growth assay showed that two different *RANBP9* WT A549 clones had a slightly higher proliferation rate and cell cycle progression than KO cells (Fig. 2a, b and S4A–B). Then, we evaluated cell viability and proliferation in response to CDDP of *RANBP9* WT and KO A549 clones. A significant reduction in total number of cells was observed after 72 h of treatment in *RANBP9* KO clones compared to *RANBP9* WT cells. For the two different KO and WT clones the average IC_{50} was 13.5 μM and 23.6 μM respectively ($p < 0.01$; Fig. 2c and S4C). Accordingly, CDDP treatment resulted in a significant reduction of colony formation by RANBP9 KO compared to WT clones (Fig. 2d and S4D).

The difference in sensitivity to CDDP was due, at least in part, to differential activation of apoptosis, as demonstrated by higher PARP cleavage (Fig. 3a and S5A), caspase 3/7 activation (Fig. 3b and S5B) and annexin-V staining in *RANBP9* KO A549 clones in comparison with WT control clones (Fig. 3c and S5C).

To test whether the absence of RANBP9 in NSCLC cells caused an increased sensitivity to cisplatin in vivo, we injected A549 *RANBP9* WT and KO cells subcutaneously into athymic nude mice. Mice bearing tumors of comparable size were randomly divided into two subgroups and treated with CDDP or vehicle. As reported in Fig. 3d, e, the ratio of tumor volume in control versus treated mice (T/C) was significantly higher in RANBP9-expressing tumors than in KO (0.77 vs. 0.27 at day 15 and 0.85 vs. 0.38 at day 19; $p < 0.05$).

Overall, these results show that the absence of RANBP9 renders NSCLC cells sensitive to platinum-based drugs both in vitro and in vivo.

RANBP9 is predictive of response to platinum in NSCLC patients

Next, we investigated the potential value of RANBP9 as prognostic and predictive biomarker in NSCLC patients. To this aim, we used specimens form a cohort of patients previously enrolled in the multicentric randomized controlled TArceva Italian Lung Optimization tRial (TAILOR) trial [22]. All patients eligible for the study had recurred or progressed after a first-line treatment with a platinum compound. A total of 132 patient specimens, collected at first diagnosis, were used to generate a TMA and evaluate RANBP9 levels by IHC. Patients demographic and characteristics are summarized in Table S4A. RANBP9 was overexpressed in the 27.3% of patients, and it correlated with high tumor stage at diagnosis (IIIb-IV vs. I-II-IIIa, $\chi^2 = 15.7$, $p < 0.0001$) and with previous adjuvant therapy ($\chi^2 = 12.6$; $p = 0.0004$; Table S4B). No correlation was found between RANBP9 expression and either age, sex, performance status (PS), history of smoke, tumor grade or histology.

After a median follow-up of 69.8 months, 63.5% of RANBP9$^{\mathbf{low}}$ (*H*-score ≤ 100 or less than 10% of cells with moderate to strong RANBP9 intensity staining) and 86.1% of patients RANBP9$^{\mathbf{high}}$ (*H*-score > 100 or at least 10% of cells with moderate to strong RANBP9 intensity staining) had died (Table S4C). The percentage of dead and/or progressed patients was 85.4 vs. 97.2 in RANBP9$^{\mathbf{low}}$ and RANBP9$^{\mathbf{high}}$ cases, respectively. The median progression free survival (PFS, defined as the time from the first-line treatment start to the date of progression or death from any cause, whichever came first) at the platinum-based first-line treatment for RANBP9$^{\mathbf{low}}$ patients was 11 months, while for RANBP9$^{\mathbf{high}}$ patients was 4.5 months (Table S4D). At the univariate analysis, the hazard ratio (HR) for RANBP9$^{\mathbf{high}}$ vs. RANBP9$^{\mathbf{low}}$ cases was 1.71 (95% CI = 1.14–2.55; $p = 0.009$). At multivariate analysis, after adjusting for sex, PS, history of smoking and histotype, RANBP9 confirmed its value as independent biomarker predictive of sensitivity to platinum in NSCLC patients (HR $_{[\text{RANBP9}^{\mathbf{high}}\ \text{vs.}\ \text{RANBP9}^{\mathbf{low}}]} = 1.73$; 95% CI = 1.15–2.59; $p = 0.008$; Fig. 4a).

Given the positive correlation of RANBP9 expression and advanced stage of disease at first disease presentation, we performed a subgroup analysis according to tumor stage at diagnosis. RANBP9 overexpression confirmed to be a negative predictive factor for sensitivity to platinum in stage I-IIIa patients (multivariate analysis HR $_{[\text{RANBP9}^{\mathbf{high}}\ \text{vs.}\ \text{RANBP9}^{\mathbf{low}}]} = 3.28$; 95% CI = 1.18–9.11; $p = 0.02$). On the contrary, RANBP9 overexpression was not significantly associated to a worse PFS in stage IIIb/IV patients (multivariate analysis HR $_{[\text{RANBP9}^{\mathbf{high}}\ \text{vs.}\ \text{RANBP9}^{\mathbf{low}}]} = 0.84$; 95% CI 0.49–1.41; $p = 0.5$).

When the overall survival (OS, defined as the time from the first-line treatment start up to the date of death from any cause) was analyzed, the HR $_{[\text{RANBP9}^{\mathbf{high}}\ \text{vs.}\ \text{RANBP9}^{\mathbf{low}}]}$ at the univariate analysis was 1.7 (95% CI 1.1–2.62; $p = 0.017$) and once the analysis has been adjusted for sex, PS, history of smoking, tumor histology and second-line treatment (erlotinib/docetaxel/patient, not randomized), the HR $_{[\text{RANBP9}^{\mathbf{high}}\ \text{vs.}\ \text{RANBP9}^{\mathbf{low}}]}$ was 1.99 (95% CI 1.27–3.11; $p = 0.003$; Fig. 4b).

All together, these data indicate that RANBP9, if validated in a prospective study, is a potential novel predictive and prognostic biomarker for the selection of NSCLC patients that would benefit from the treatment with platinum compounds.

Ablation of RANBP9 impairs ATM activation and results in increased levels of chromatin-bound PARylated proteins

RANBP9 is a target and a facilitator of the ATM kinase and its silencing in NSCLC cells causes deficits of the HDR after IR exposure [20, 21]. We tested whether A549 cells in which RANBP9 is genetically ablated showed deficiencies of the ATM-dependent DDR pathway leading to HDR in response to cisplatin (Fig. 5a). In comparison to controls, *RANBP9* KO cells showed a reduced activation of ATM (S1981), Chk2 (T68) and p53 (S15). Also, higher overall levels of p53 were observed in WT vs. KO cells, likely due to increased protein stability of phosphorylated p53.

In NSCLC cells the ATM/Chk2 pathway stimulation results in a significant activation of the late-S/early-G2-phase checkpoint [24, 25]. However, we observed that *RANBP9* KO cells accumulated in the S-phase of the cell cycle (Fig. 5b) in comparison to RANBP9 WT controls, suggesting that the ablation of RANBP9 causes NSCLC cells to activate different cell-cycle checkpoints to cope with genotoxic stress.

We also found that the absence of RANBP9 affects specifically the ATM-dependent but not the insulin-dependent activation of AKT, a well-known regulator of cell survival upon stress (Fig. 5c).

When one DDR mechanism is impaired, cancer cells become dependent on alternative repair players [26, 27] such as Poly(ADP-ribose) Polymerase 1 (PARP1) [28, 29]. For this reason, we assessed the status of PARP activation in RANBP9 WT and KO cells. As shown in Fig. 5d, *RANBP9* KO cells showed higher amounts of PARylated chromatin-bound proteins in comparison with WT cells, both at the basal level and after treatment with CDDP. Accordingly, *RANBP9* WT cells showed an increase in phosphorylated H2AX (gamma-H2AX), a target of ATM during HDR-mediated DNA repair, after platinum exposure. Conversely, in *RANBP9* KO cells, gamma-H2AX levels were not altered by treatment with platinum.

These data indicate that the loss of RANBP9 causes an increase of PARylated proteins bound to the chromatin of NSCLC cells.

RANBP9 ablation enhances NSCLC cells sensitivity to PARP inhibitors alone and in combination with CDDP

To investigate whether RANBP9 absence affected NSCLC sensitivity to PARPi, we treated A549 WT and KO clones with AZD2281 (olaparib). *RANBP9* KO cells were significantly less in numbers and formed also significantly fewer colonies than controls in response to olaparib (Fig. 6a–c and S6A–C).

PARPi generate different types of DNA damage, ultimately resulting in DNA DSBs [30, 31]. Thus, we evaluated the effect of RANBP9 ablation on H2AX phosphorylation and DNA

repair by HDR following exposure of cells to olaparib. As shown in Fig. 6d, e and S6D–E, olaparib was able to induce γH2AX foci in *RANBP9* WT cells while they were almost absent in KO cells.

Finally, we tested the effects of CDDP and olaparib combination. Overall, RANBP9 KO cells displayed reduced growth and increased late-apoptosis activation in comparison with WT cells upon treatment with CDDP, olaparib or the combination of the two drugs (Fig. 6f, g and S6F).

In summary, these results indicate that RANBP9 KO NSCLC cells rely on PARP-dependent mechanisms for DNA repair to cope with both basal and CDDP-induced genotoxic stress. Moreover, inhibition of PARP in the absence of RANBP9 results in reduced NSCLC cell proliferation and enhanced apoptosis alone or in combination with CDDP.

Discussion

NSCLC patients are mostly treated with platinum-based drugs [4]. Since the main mechanism of action of platinum compounds is based on induction of DNA damage, a full understanding and appropriate knowledge of the DDR is crucial.

Previous studies showed that RANBP9 is critical for DNA double-strand breaks repair in NSCLC cells [20]. For this reason, we aimed to investigate the clinical relevance of these observations and the possible role of RANBP9 in the treatment of NSCLC patients.

An IHC survey performed on a total of 147 samples (Fig. 1, Table S1–S2) unequivocally shows that LC malignancies have increased levels of RANBP9 in comparison with NATs, independently of the histotype. This observation is in agreement with data from the COSMIC and TGCA databases clearly indicating that RANBP9 is overexpressed in NSCLC (Figure S1A–B). Furthermore, high amounts of RANBP9 are maintained or increased in nodal metastases compared to primary tumors (Fig. 1) suggesting a positive role of RANBP9 in LC progression.

Up-to-date, mostly in vitro evidence suggested that RANBP9 might have tumor suppressive functions [18, 19, 32–36]. However, RANBP9 appears to be rarely mutated and mostly overexpressed rather than downregulated in all types of cancers (Table S3). A recent analysis of a cohort of stage I and II LC patients suggested a positive correlation of higher levels of RANBP9 mRNA with better LC prognosis [37] in apparent contrast with our current findings. However, this latter study was exclusively based on mRNA expression and highly biased for early stage cases. In fact, the analysis of the entire LC TCGA collection does not show any significant correlation between RANBP9 mRNA levels and clinical outcome (not shown). In the current study, we observed in vitro and ex vivo (Figure S1C–D and S2B–C) that RANBP9 protein and mRNA levels does not always positively correlate, in agreement with well-known observations especially for proteins involved in cellular stress response [38–40]. For this reason, we decided to rely on and further validate (Figure S2) an IHC reagent approved by the Human Protein Atlas Project, using multiple techniques (western blot and IHC).

Other than establishing increased expression at late stages, our study focuses on the role of RANBP9 in response to genotoxic therapies. However, it is tempting to speculate that RANBP9, similarly to other DDR players, might display both pro- and anti-tumorigenic functions, depending on multiple factors such as the cellular context, the molecular partners and the tumorigenesis status. In fact, although proteins involved in DNA repair prevent accumulation of DNA damage and cellular transformation [41, 42], their overexpression is associated with resistance to genotoxic treatments [43]. Taken together, these observations highlight the need for the generation of models of NSCLC for systematic in vivo studies to elucidate the role of RANBP9 in different steps of lung tumorigenesis.

Regarding the clinical relevance of our findings, it was previously shown that NSCLC cell lines silenced for RANBP9 were more sensitive to ionizing radiation and CDDP [20]. Here, we generated complete *RANBP9* KO NSCLC cell lines to maximize the detection of a cellular phenotype. In agreement with previous results, abrogation of RANBP9 caused an impairment of HDR-based DDR to genotoxic treatments both in vitro and in vivo (Figs. 2, 3, 5, 6 and S3–5). Of note, the variations in sensitivity in the presence or absence of RANBP9 observed in our in vitro and in vivo studies are quantitatively in the same range as for other previously reported cisplatin-sensitizing proteins (~2 folds, depending on the cell type analyzed) [44, 45]. Prompted by this observation, we measured RANBP9 protein levels on a cohort of NSCLC patients from the TAILOR study [22] that had undergone a first-line platinum-based treatment. In those patients, higher levels of RANBP9 correlated with lower OS and PFS (Fig. 4a, b), in accordance with and further supporting the relevance of the data obtained in vitro. However, it has to be considered that the influence of RANBP9 expression on OS can only be partially evaluated, since patients from the TAILOR study underwent multiple second-line treatments including either docetaxel or erlotinib. Relevant to this limitation in our study, it has been demonstrated that, while abrogation/ deficiency of the ATM-dependent pathways (including the ATM-MDC1-BRCA1/RAP80/ABRAXAS pathway) enhances the sensitivity to platinum-based drugs, the opposite effect is observed in response to microtubule-targeting agents [46–48].

When genes involved in HDR are lost or mutated, the use of PARP inhibitors (PARPi) blocks the ability of cancer cells to repair DNA damages through alternative pathways (i.e., PARP-dependent DNA repair), resulting in “synthetic lethality” [30, 49]. In certain tumor types such as ovarian cancer, somatic alterations in *BRCA1* or *BRCA2* genes result in a dramatic defect of HDR (frequently reported as “BRCAness phenotype”), making cancer cells dependent on PARP activity [49]. The use of PARPi in cells showing a BRCAness phenotype causes cancer cell death due to synthetic lethality, which is one of the most promising approaches in exploiting the DNA-repair deficiency in the clinic [43]. However, *BRCA* germline or somatic mutations in NSCLC have only rarely been described [50]. On the other hand, it is now accepted that a BRCAness-like phenotype can be the result of genetic and epigenetic changes other than mutations of the two BRCA genes [51]. Thus, in order to identify NSCLC patients that could benefit from PARPi, biomarkers of dysfunctional HDR need to be identified and tested. Here we show that RANBP9 KO cells displayed increased amount of chromatin-bound PARylated proteins, possibly as a compensatory mechanism to cope with genotoxic stress. Accordingly, in the absence of RANBP9, NSCLC cell lines became significantly more sensitive to PARP targeting using

olaparib. This result supports the potential use of RANBP9 as a biomarker of a “BRCAness-like” phenotype to identify NSCLC patients that might benefit from therapies with PARP-targeting agents (Fig. 7). Future studies will be required to assess the potential involvement of RANBP9 in other known mechanisms of resistance/sensitivity to PARP inhibitors, such as those involving components of ATR pathway, receptor tyrosine kinases or the putative RNA/DNA helicase SLFN11 [52–54]. In summary, the present study provides preclinical and clinical data indicating that lower RANBP9 protein levels might be used, after perspective validation, as a biomarker predictive of response to platinum based compounds. However, the retrospective nature of the current study limits our conclusions to the association between RANBP9 protein levels and clinical outcome of NSCLC. Nonetheless, our results pave the way to future prospective clinical studies in NSCLC patients, using RANBP9 levels to evaluate the potential benefit of PARP inhibitors, a class of compounds still lacking a reliable predictive biomarker in LC patients. Finally, our data also suggest RANBP9 inhibition as a new potential strategy for targeting the DDR in NSCLC patients.

Supplementary Material

Refer to Web version on PubMed Central for supplementary material.

Acknowledgements

Authors are thankful to Dr. R. Shakya and the Target Validation Shared Resource, the Campus Microscopy & Imaging Facility, the Analytical Cytometry Shared Resource, the Comparative Pathology and Mouse Phenotyping Shared Resource, the Genetically Engineered Mouse Modeling Core, and N. Single and L. Monovich of the Biospecimen Services Shared Resource of the Ohio State University-Comprehensive Cancer Center. A.T. and M.P. are recipients of a Pelotonia Fellowship for Cancer Research. This work was supported by start-up funds to V.C. from the College of Medicine, Office of Research, and Comprehensive Cancer Center of the Ohio State University.

References

1. Kris MG, Gaspar LE, Chaft JE, Kennedy EB, Azzoli CG, Ellis PM et al. Adjuvant systemic therapy and adjuvant radiation therapy for stage I to IIIA completely resected non-small-cell lung cancers: American Society of Clinical Oncology/Cancer Care Ontario Clinical Practice Guideline Update. J Clin Oncol. 2017: JCO2017724401.
2. Pisters KM, Evans WK, Azzoli CG, Kris MG, Smith CA, Desch CE, et al. Cancer Care Ontario and American Society of Clinical Oncology adjuvant chemotherapy and adjuvant radiation therapy for stages I-IIIA resectable non small-cell lung cancer guideline. J Clin Oncol. 2007;25:5506–18. [PubMed: 17954710]
3. Chan BA, Hughes BG. Targeted therapy for non-small cell lung cancer: current standards and the promise of the future. Transl Lung Cancer Res. 2015;4:36–54. [PubMed: 25806345]
4. Xiong Y, Huang BY, Yin JY. Pharmacogenomics of platinum-based chemotherapy in non-small cell lung cancer: focusing on DNA repair systems. Med Oncol. 2017;34:48. [PubMed: 28215024]
5. Shukuya T, Carbone DP. Predictive markers for the efficacy of anti-PD-1/PD-L1 antibodies in lung cancer. J Thorac Oncol. 2016;11:976–88. [PubMed: 26944305]
6. Kuribayashi K, Funaguchi N, Nakano T. Chemotherapy for advanced non-small cell lung cancer with a focus on squamous cell carcinoma. J Cancer Res Ther. 2016;12:528–34. [PubMed: 27461605]
7. Swift LH, Golsteyn RM. Genotoxic anti-cancer agents and their relationship to DNA damage, mitosis, and checkpoint adaptation in proliferating cancer cells. Int J Mol Sci. 2014;15:3403–31. [PubMed: 24573252]

8. Socinski MA, Jotte RM, Cappuzzo F, Orlandi F, Stroyakovskiy D, Nogami N, et al. Atezolizumab for first-line treatment of metastatic nonsquamous NSCLC. N Engl J Med. 2018;378:2288–301. [PubMed: 29863955]
9. Socinski MA, Obasaju C, Gandara D, Hirsch FR, Bonomi P, Bunn PA Jr, et al. Current and emergent therapy options for advanced squamous cell lung cancer. J Thorac Oncol. 2018;13:165–83. [PubMed: 29175116]
10. Kelland L The resurgence of platinum-based cancer chemotherapy. Nat Rev Cancer. 2007;7:573–84. [PubMed: 17625587]
11. Woods D, Turchi JJ. Chemotherapy induced DNA damage response: convergence of drugs and pathways. Cancer Biol Ther. 2013;14:379–89. [PubMed: 23380594]
12. Arafa HM, Abdel-Hamid MA, El-Khouly AA, Elmazar MM, Osman AM. Enhancement by dexamethasone of the therapeutic benefits of cisplatin via regulation of tumor angiogenesis and cell cycle kinetics in a murine tumor paradigm. Toxicology. 2006;222:103–13. [PubMed: 16567030]
13. Brouwers EE, Huitema AD, Beijnen JH, Schellens JH. Long-term platinum retention after treatment with cisplatin and oxaliplatin. BMC Clin Pharmacol. 2008;8:7. [PubMed: 18796166]
14. Chaudhary UB, Haldas JR. Long-term complications of chemotherapy for germ cell tumours. Drugs. 2003;63:1565–77. [PubMed: 12887263]
15. Drottar M, Liberman MC, Ratan RR, Roberson DW. The histone deacetylase inhibitor sodium butyrate protects against cisplatin-induced hearing loss in guinea pigs. Laryngoscope. 2006;116:292–6. [PubMed: 16467722]
16. Hatzopoulos S, Di Stefano M, Albertin A, Martini A. Evaluation of cisplatin ototoxicity in a rat animal model. Ann NY Acad Sci. 1999;884:211–25. [PubMed: 10842595]
17. Lee SM, Falzon M, Blackhall F, Spicer J, Nicolson M, Chaudhuri A, et al. Randomized prospective biomarker trial of ERCC1 for comparing platinum and nonplatinum therapy in advanced non-small-cell lung cancer: ERCC1 Trial (ET). J Clin Oncol. 2017;35:402–11. [PubMed: 27893326]
18. Salemi LM, Maitland MER, McTavish CJ, Schild-Poulter C. Cell signalling pathway regulation by RanBPM: molecular insights and desease implications. Open Biol. 2017;7:170081. [PubMed: 28659384]
19. Suresh B, Ramakrishna S, Baek KH. Diverse roles of the scaffolding protein RanBPM. Drug Discov Today. 2012;17:379–87. [PubMed: 22094242]
20. Palmieri D, Scarpa M, Tessari A, Uka R, Amari F, Lee C, et al. Ran Binding Protein 9 (RanBP9) is a novel mediator of cellular DNA damage response in lung cancer cells. Oncotarget. 2016;7:18371–83. [PubMed: 26943034]
21. Yard BD, Adams DJ, Chie EK, Tamayo P, Battaglia JS, Gopal P, et al. A genetic basis for the variation in the vulnerability of cancer to DNA damage. Nat Commun. 2016;7:11428. [PubMed: 27109210]
22. Garassino MC, Martelli O, Broggini M, Farina G, Veronese S, Rulli E, et al. Erlotinib versus docetaxel as second-line treatment of patients with advanced non-small-cell lung cancer and wild-type EGFR tumours (TAILOR): a randomised controlled trial. Lancet Oncol. 2013;14:981–8. [PubMed: 23883922]
23. Kellar A, Egan C, Morris D. Preclinical Murine Models for Lung Cancer: Clinical Trial Applications. Biomed Res Int. 2015;2015:621324 [PubMed: 26064932]
24. Horibe S, Matsuda A, Tanahashi T, Inoue J, Kawauchi S, Mizuno S. et al. Cisplatin resistance in human lung cancer cells is linked with dysregulation of cell cycle associated proteins. Life Sci. 2015;124:31–40. [PubMed: 25625243]
25. Sears CR, Cooney SA, Chin-Sinex H, Mendonca MS, Turchi JJ. DNA damage response (DDR) pathway engagement in cisplatinradiosensitization of non-small cell lung cancer. DNA Repair. 2016;40:35–46. [PubMed: 26991853]
26. Ceccaldi R, Liu JC, Amunugama R, Hajdu I, Primack B, Petalcorin MI. et al. Homologous-recombination-deficient tumours aredependent on Poltheta-mediated repair. Nature. 2015;518:258–62. [PubMed: 25642963]

27. Konstantinopoulos PA, Ceccaldi R, Shapiro GI, D'Andrea AD. Homologous recombination deficiency: exploiting the fundamental vulnerability of ovarian cancer. Cancer Discov. 2015;5:1137–54. [PubMed: 26463832]
28. Eustermann S, Wu WF, Langelier MF, Yang JC, Easton LE, Riccio AA. et al. Structural basis of detection and signaling of DNA single-strand breaks by human PARP-1. Mol Cell. 2015;60:742–54. [PubMed: 26626479]
29. Satoh MS, Lindahl T. Role of poly (ADP-ribose) formation in DNA repair. Nature. 1992;356:356–8. [PubMed: 1549180]
30. Bryant HE, Schultz N, Thomas HD, Parker KM, Flower D, Lopez E. et al. Specific killing of BRCA2-deficient tumours with inhibitorsof poly(ADP-ribose) polymerase. Nature. 2005;434:913–7. [PubMed: 15829966]
31. Murai J, Huang SY, Das BB, Renaud A, Zhang Y, Doroshow JH. et al. Trapping of PARP1 and PARP2 by clinical PARP inhibitors. Cancer Res. 2012;72:5588–99. [PubMed: 23118055]
32. Atabakhsh E, Bryce DM, Lefebvre KJ, Schild-Poulter C. RanBPM has proapoptotic activities that regulate cell death pathways inresponse to DNA damage. Mol Cancer Res.2009;7:1962–72. [PubMed: 19996306]
33. Atabakhsh E, Schild-Poulter C. RanBPM is an inhibitor of ERK signaling. PLoS ONE. 2012;7:e47803. [PubMed: 23118896]
34. Shao S, Sun PH, Satherley LK, Gao X, Ji KE, Feng YI, et al. Reduced RanBPM expression is associated with distant metastasis in gastric cancer and chemoresistance. Anticancer Res. 2016;36:1295–303. [PubMed: 26977028]
35. Suresh B, Ramakrishna S, Kim YS, Kim SM, Kim MS, Baek KH. Stability and function of mammalian lethal giant larvae-1 oncoprotein are regulated by the scaffolding protein RanBPM. J Biol Chem. 2010;285:35340–9. [PubMed: 20829363]
36. Zhu LL, Wang CH, Yang HP, Shu WH. Expression of cartilage antitumor component RanBP9 in osteosarcoma. J Biol Regul Homeost Agents. 2016;30:103–10.
37. Zhao Z, Cheng S, Zabkiewicz C, Chen J, Zhang L, Ye L, et al. Reduced expression of RanBPM is associated with poorer survival from lung cancer and increased proliferation and invasion of lung cancer cells in vitro. Anticancer Res. 2017;37:4389–97. [PubMed: 28739732]
38. Hoernes TP, Huttenhofer A, Erlacher MD. mRNA modifications: dynamic regulators of gene expression? RNA Biol. 2016;13:760–5. [PubMed: 27351916]
39. Liu Y, Beyer A, Aebersold R. On the dependency of cellular protein levels on mRNA abundance. Cell. 2016;165:535–50. [PubMed: 27104977]
40. Vogel C, Marcotte EM. Insights into the regulation of protein abundance from proteomic and transcriptomic analyses. Nat Rev Genet. 2012;13:227–32. [PubMed: 22411467]
41. Ghosal G, Chen J. DNA damage tolerance: a double-edged sword guarding the genome. Transl Cancer Res. 2013;2:107–29. [PubMed: 24058901]
42. Pawlowska E, Blasiak J. DNA repair--a double-edged sword in the genomic stability of cancer cells--the case of chronic myeloid leukemia. Int J Mol Sci. 2015;16:27535–49. [PubMed: 26593906]
43. Postel-Vinay S, Vanhecke E, Olaussen KA, Lord CJ, Ashworth A, Soria JC. The potential of exploiting DNA-repair defects for optimizing lung cancer treatment. Nature reviews. Clin Oncol (R Coll Radiol). 2012;9:144–55.
44. Jin HO, Hong SE, Woo SH, Lee JH, Choe TB, Kim EK, et al. Silencing of Twist1 sensitizes NSCLC cells to cisplatin via AMPK-activated mTOR inhibition. Cell Death Dis. 2012;3:e319. [PubMed: 22673193]
45. Leung AWY, Veinotte CJ, Melong N, Oh MH, Chen K, Enfield KSS, et al. In vivo validation of PAPSS1 (3'-phosphoadenosine 5'-phosphosulfate synthase 1) as a cisplatin-sensitizing therapeutic target. Clin Cancer Res. 2017;23:6555–66. [PubMed: 28790117]
46. Bonanno L Predictive models for customizing chemotherapy in advanced non-small cell lung cancer (NSCLC). Transl Lung Cancer Res. 2013;2:160–71. [PubMed: 25806229]
47. Quinn JE, Kennedy RD, Mullan PB, Gilmore PM, Carty M, Johnston PG, et al. BRCA1 functions as a differential modulator of chemotherapy-induced apoptosis. Cancer Res. 2003;63:6221–8. [PubMed: 14559807]

48. Rosell R, Skrzypski M, Jassem E, Taron M, Bartolucci R, Sanchez JJ, et al. BRCA1: a novel prognostic factor in resected non-small-cell lung cancer. PLoS ONE. 2007;2:e1129. [PubMed: 17987116]

49. Farmer H, McCabe N, Lord CJ, Tutt AN, Johnson DA, Richardson TB, et al. Targeting the DNA repair defect in BRCA mutant cells as a therapeutic strategy. Nature. 2005;434:917–21. [PubMed: 15829967]

50. Turner N, Tutt A, Ashworth A. Hallmarks of 'BRCAness' in sporadic cancers. Nat Rev Cancer. 2004;4:814–9. [PubMed: 15510162]

51. Lord CJ, Ashworth A. BRCAness revisited. Nat Rev Cancer. 2016;16:110–20. [PubMed: 26775620]

52. Ballestrero A, Bedognetti D, Ferraioli D, Franceschelli P, Labidi-Galy SI, Leo E, et al. Report on the first SLFN11 monothematic workshop: from function to role as a biomarker in cancer. J Transl Med. 2017;15:199. [PubMed: 28969705]

53. Chen MK, Hung MC. Regulation of therapeutic resistance in cancers by receptor tyrosine kinases. Am J Cancer Res. 2016;6:827–42. [PubMed: 27186434]

54. Reinhold WC, Thomas A, Pommier Y. DNA-targeted precision medicine; have we been caught sleeping? Trends Cancer. 2017;3:2–6. [PubMed: 28603778]

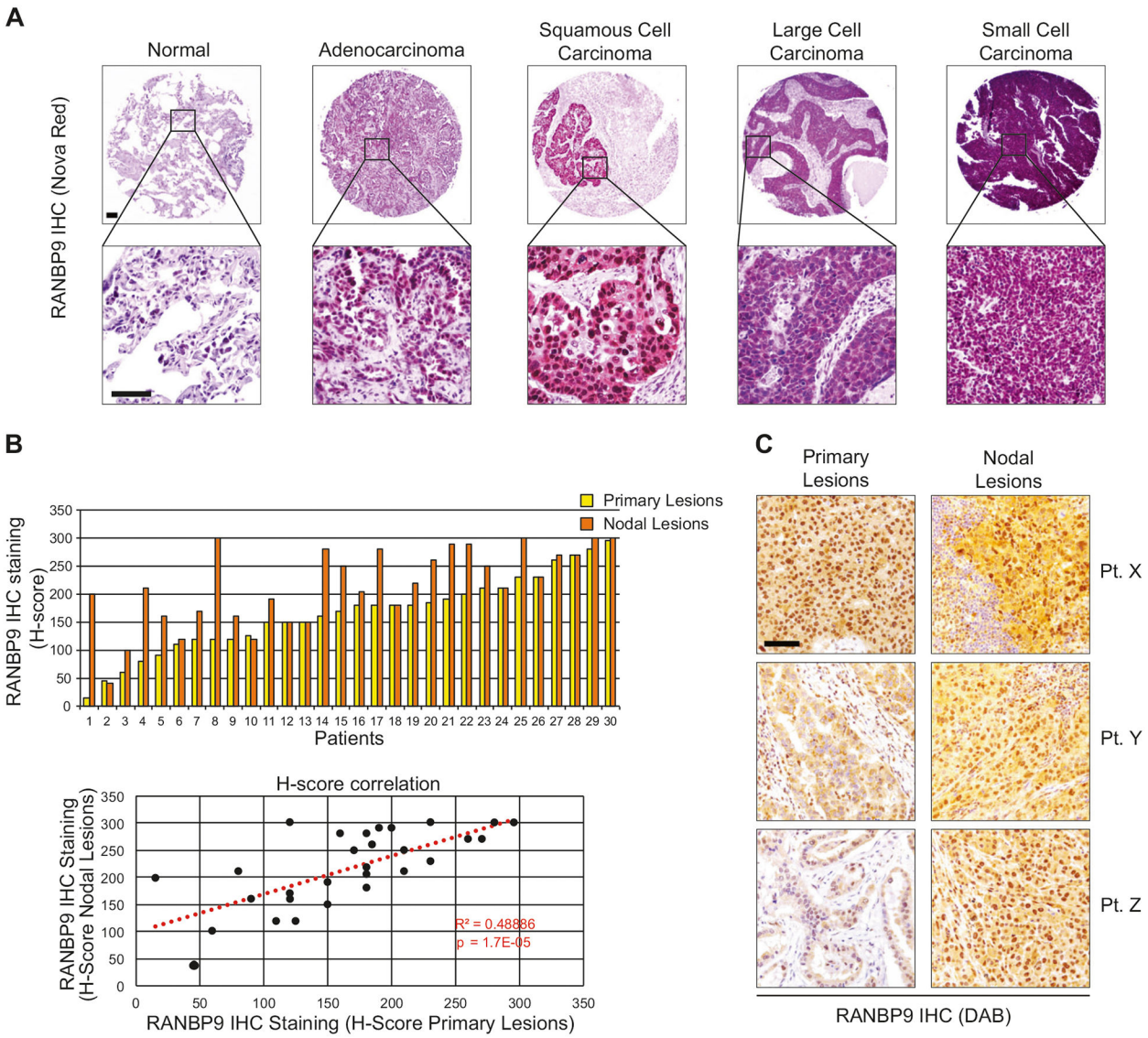

Fig. 1.

RANBP9 is overexpressed in lung cancer primary tumors and nodal metastases. **a** Representative examples of RANBP9 expression evaluated by IHC (Nova Red staining) in different histotypes of lung cancer and in normal adjacent tissue (NAT). Scale bars represent 100 μm. **b** Upper panel: RANBP9 protein levels evaluated by IHC in 30 cases of NSCLC primary tumors (yellow bars) and corresponding nodal metastasis (orange bars). Lower panel: positive correlation of RANBP9 protein levels between the primary lung adenocarcinomas and the nodal lesions ($R^2 = 0.48886$; $p < 0.001$). The correlation was calculated according to Pearson correlation coefficient. Trend is indicated by a red dotted line. **c** Representative examples of RANBP9 expression in primary tumors and in the corresponding nodal lesions evaluated by IHC (DAB staining) in three different, representative patient specimens. Scale bars represent 100 μm

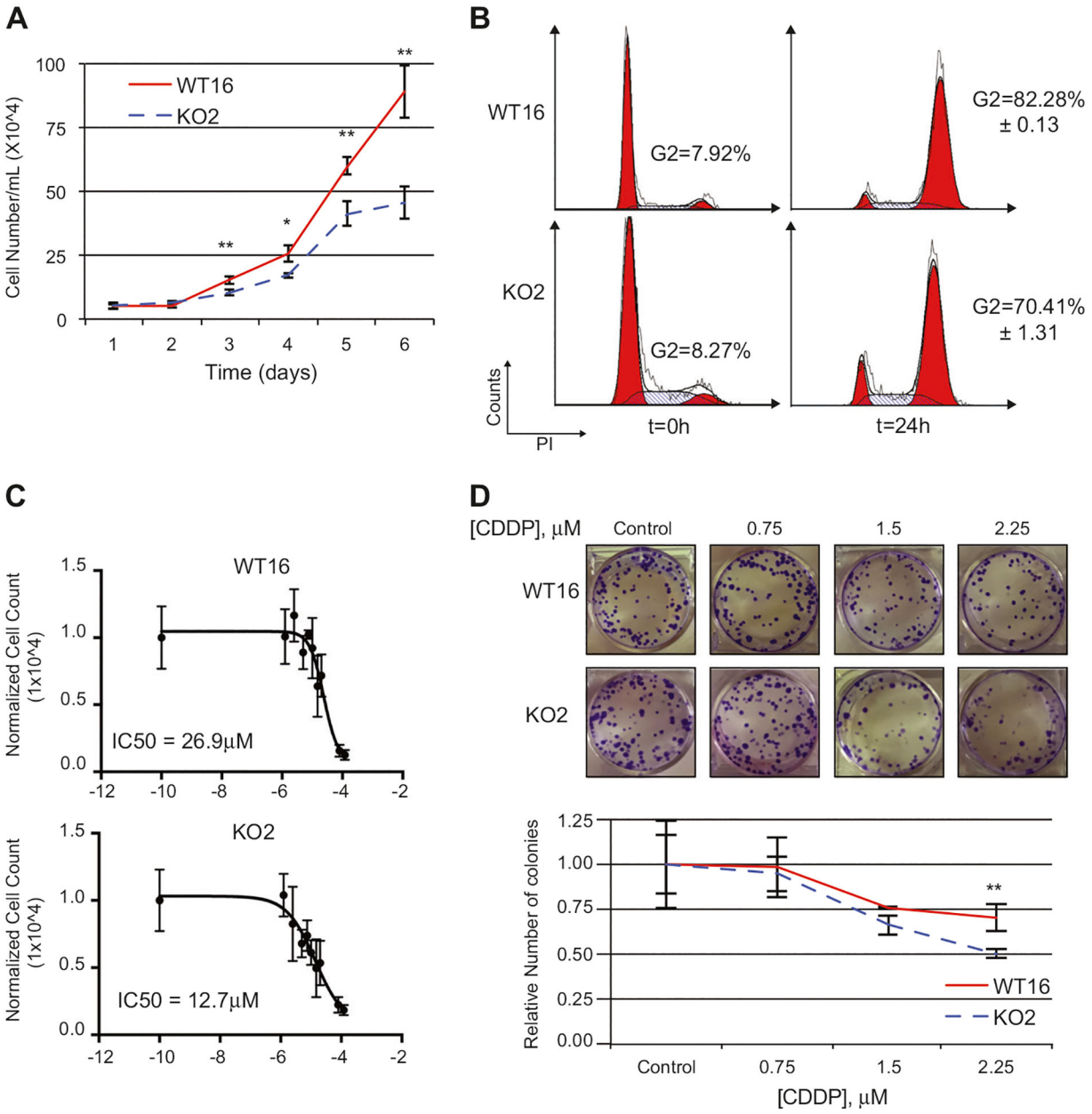

Fig. 2.

Effects of RANBP9 abrogation on NSCLC cells proliferation and sensitivity to cisplatin. **a** Growth curve of *RANBP9* WT and KO clones showing the lower proliferation rate of cells lacking in RANBP9 expression. Data are representative of two independent experiments performed in triplicate. **b** Cell cycle analysis by flow cytometry of propidium iodide stained cells. Red peaks indicate G1 and G2 phase, stripes indicate S phase. Cells were treated with nocodazole 200 ng/mL for 24 h to induce G2-blockage in order to identify the percentage of cells moving from G1 to G2 phase. Data are representative of two independent experiments. **c** CDDP IC50 calculation on *RANBP9* WT16 (C, IC50: 26.9 µM) and KO2 (D, IC50: 12.7 µM) clones. Data are representative of two independent experiments. **d** Colony assay and quantification of A549 *RANBP9* WT and KO clones left untreated (NT) or treated with the

indicated dose of CDDP for 24 h. Cells were allowed to grow for 8 days and then colonies were stained and counted. The average colony number normalized for the NT ± SD is reported. *p-value < 0.05, **p-value < 0.01. Data are representative of two independent experiments performed in triplicate

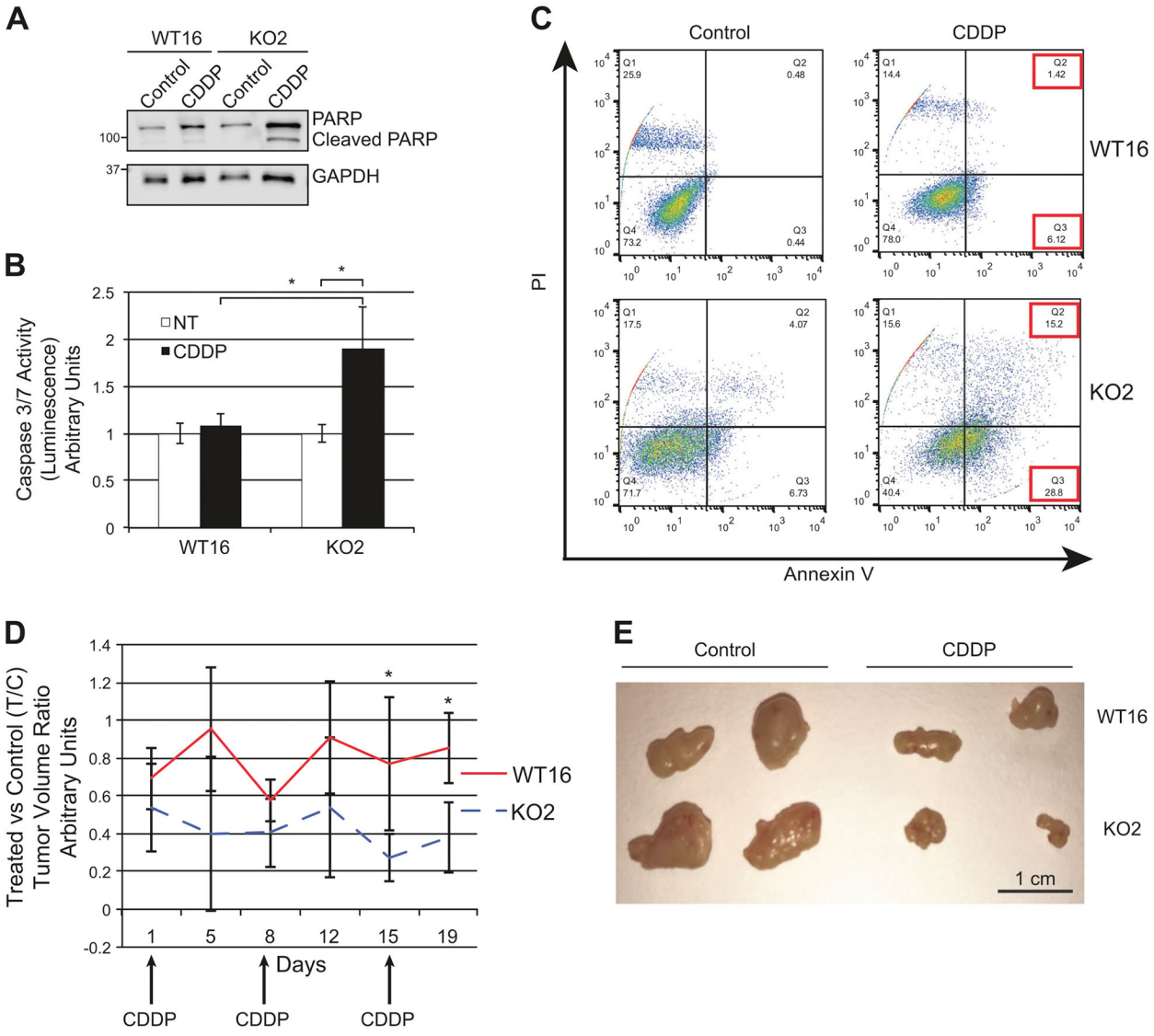

Fig. 3.

RANBP9 KO are more sensitive to cisplatin than *RANBP9* WT NSCLC cells both in vitro and in vivo. **a** Western blot analysis of *RANBP9* WT and KO A549 clones, treated for 24 h with 15 μM CDDP to evaluate total and cleaved PARP. GAPDH was used as loading control. **b** Caspase 3/7 activation assay performed on A549 *RANBP9* WT and KO clones. Cells were left untreated or treated with CDDP 15 μM for 24 h. *$p < 0.05$. Data are representative of three independent experiments performed in triplicate. **c** Flow cytometry analysis of RANBP9 WT and KO cells left untreated or treated with CDDP 20 μM for 72 h, and stained with propidium iodide (PI) and Annexin V-FITC. Data are representative of two independent experiments. **d** NOD-SCID mice ($n = 8$) were subcutaneously injected with 5×10^6 A549 *RANBP9* WT and KO on the left and right flank, respectively. Once the tumors were detectable, mice were treated with control solution ($n = 4$) or 5 mg/kg of CDDP ($n = 4$), once a week for three weeks. Mice were monitored and tumors were measured by physical examination twice a week. After 19 days from the first injection, mice were euthanized.

Tumors were excised and measured. CDDP-treated versus control-treated tumor volume ratios (T/C) ± S.D. are reported. *p-value < 0.05. e Representative image of *RANBP9* WT and KO tumors, treated with CDDP and vehicle control treated

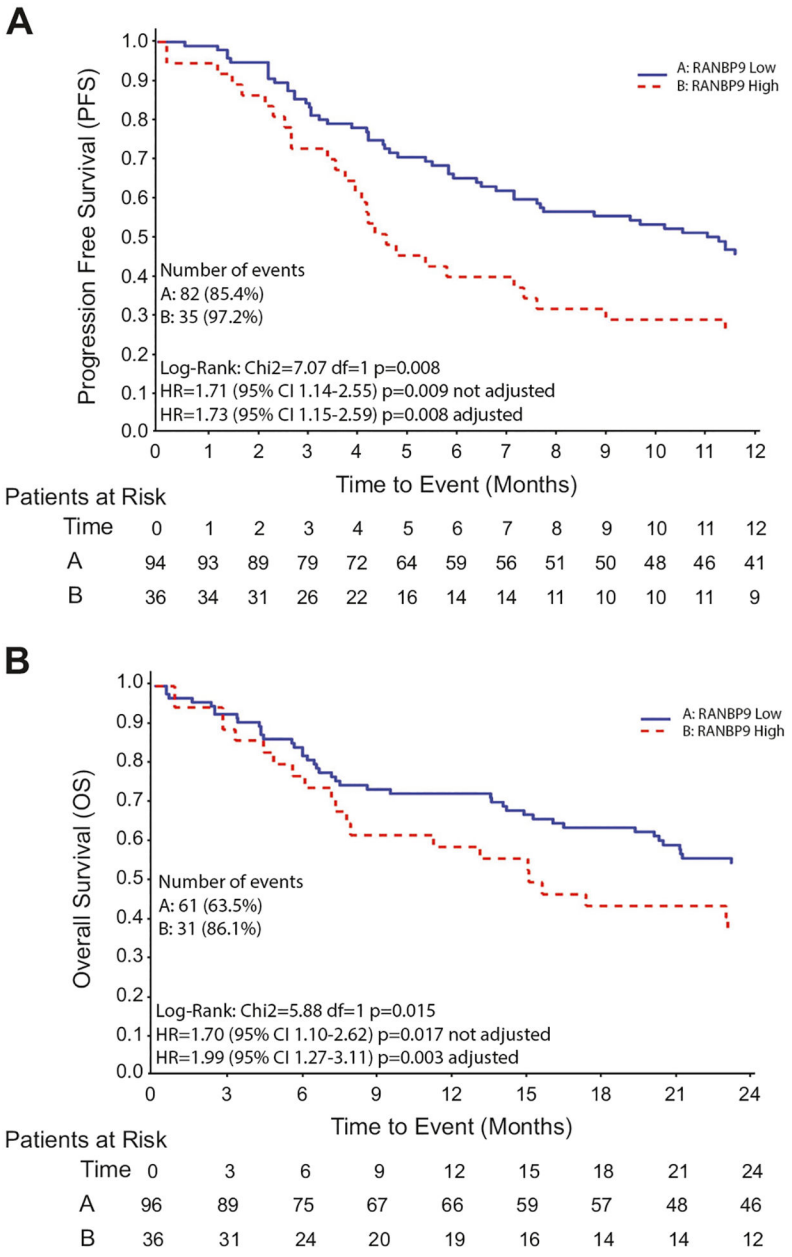

Fig. 4.

RANBP9 levels are predictive of response to platinum in NSCLC patients. **a** Kaplan–Meier curves representing the progression free survival (PFS) of RANBP9-low (blue line) and -high (red line) NSCLC patients treated with platinum compound as first-line. **b** Kaplan–Meier curves representing the overall survival (OS) of the same population as in (**a**)

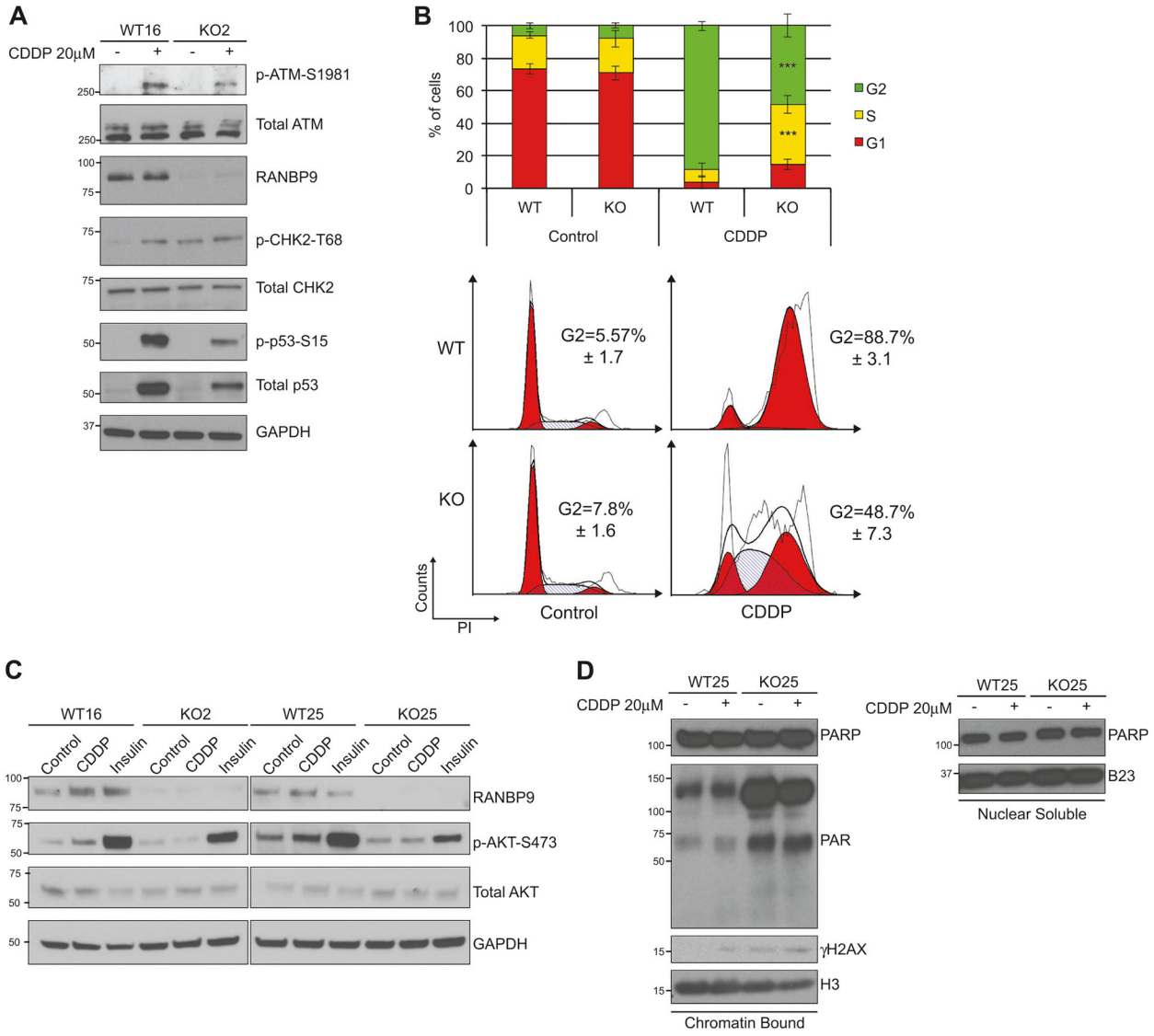

Fig. 5.

RANBP9 ablation impairs ATM activation and results in increased amounts of chromatin-bound PARylated proteins. **a** WB analysis of *RANBP9* WT and KO clones left untreated or after 24 h of treatment with 20 μM CDDP, using the indicated antibodies. GAPDH was used as loading control. **b** Cell cycle analysis by flow cytometry of propidium iodide stained *RANBP9* WT and KO cells, not treated or treated with 30 μM CDDP for 48 h. Red peaks indicate G1 and G2 phase, stripes indicate S phase. After the treatment with the platinum compound, *RANBP9* WT cells exhibit G2 phase blockage, while RANBP9 KO clones are blocked in S phase. **c** WB analysis of *RANBP9* WT and KO clones left untreated or after 24 h of treatment with 20 μM CDDP or 30 min of 100 nM insulin using the indicated antibodies. GAPDH was used as loading control. **d** PARylation levels in *RANBP9* WT and KO clones after the treatment with CDDP evaluated by Western blot. Cells were left untreated or exposed to 20 μM CDDP for 30 min. Then chromatin bound and nuclear

soluble fractionated proteins were extracted. Histone H3 was used as loading control for chromatin bound fraction, nucleophosmin (B23) for nuclear soluble proteins

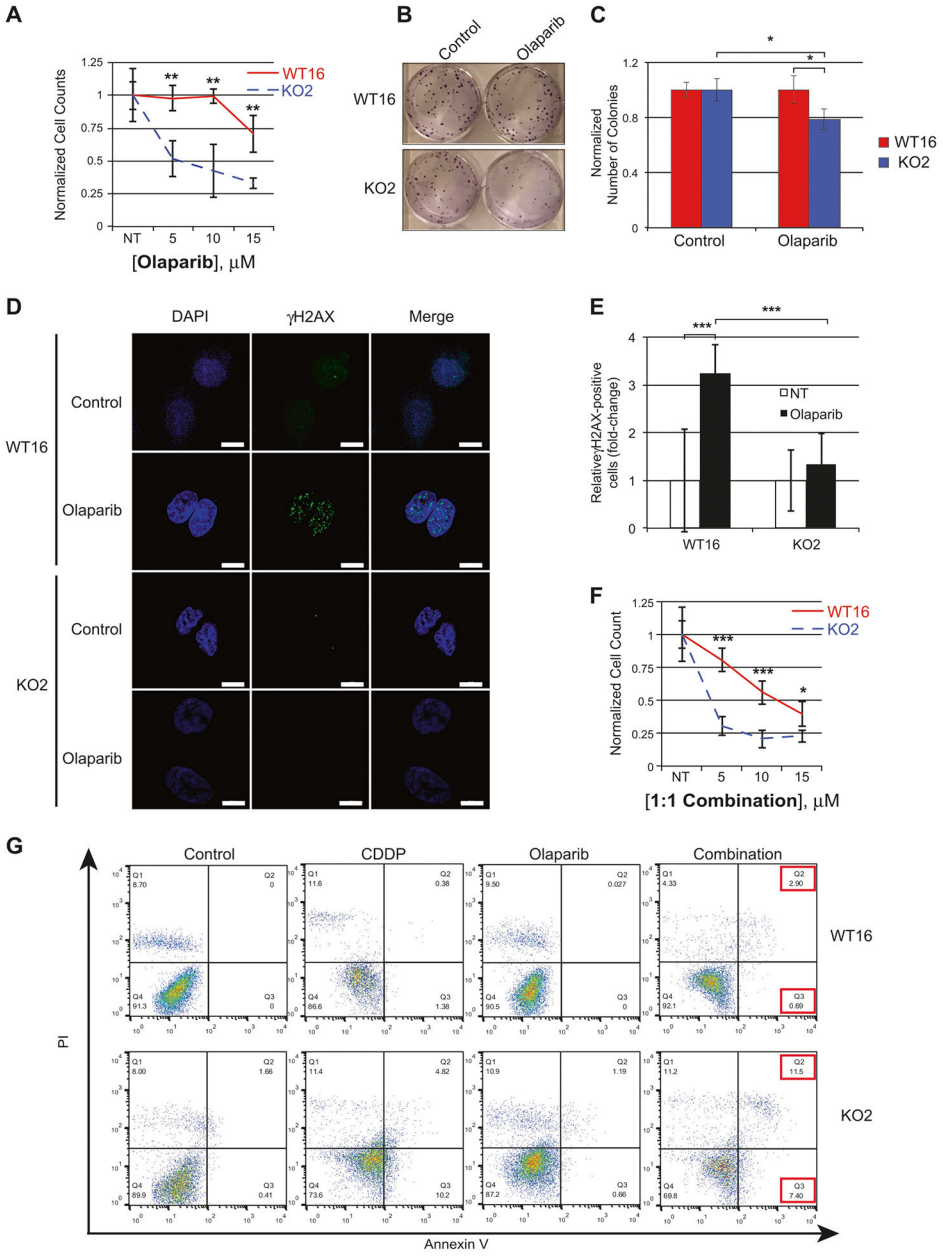

Fig. 6.

RANBP9 KO cells are more sensitive to PARP inhibition alone and in combination with CDDP. **a** Cell survival after 72 h of treatment with increasing doses of olaparib on *RANBP9* WT and KO clones. Data are representative of three independent experiments. **b**, **c** Colony assay and quantitation on A549 *RANBP9* WT and KO clones left untreated (NT) or treated with olaparib 5 μM for 24 h. Cells were grown for 8 days and then colonies were stained with crystal violet and counted. The average colony number normalized for the NT ± SD is reported. **p*-value < 0.05, ***p*-value < 0.01, ****p*-value < 0.001. **d** Activation of the ATM-dependent DDR leading to H2AX phosphorylation, evaluated by immunofluorescence. Cells were left untreated (NT) or treated with 10 μM olaparib for 7 h. Scale bars represent 10 μm. e Quantification of the experiment in (**d**) of γH2AX positive cells (cells with >=10 foci). At

least 100 cells counted each condition. Data are representative of three independent experiments. ***p-value < 0.001. **f** Cell survival of *RANBP9* WT and KO clones after 72 h of treatment with incremental doses of 1:1 CDDP:olaparib in combination. Data are representative of three independent experiments. g Flow cytometry analysis of *RANBP9* WT and KO cells left untreated (NT) or treated with either 20 μM CDDP, 30 μM olaparib or the combination of the two drugs for 6 days, then stained with propidium iodide (PI) and Annexin V-FITC. Data are representative of two independent experiments

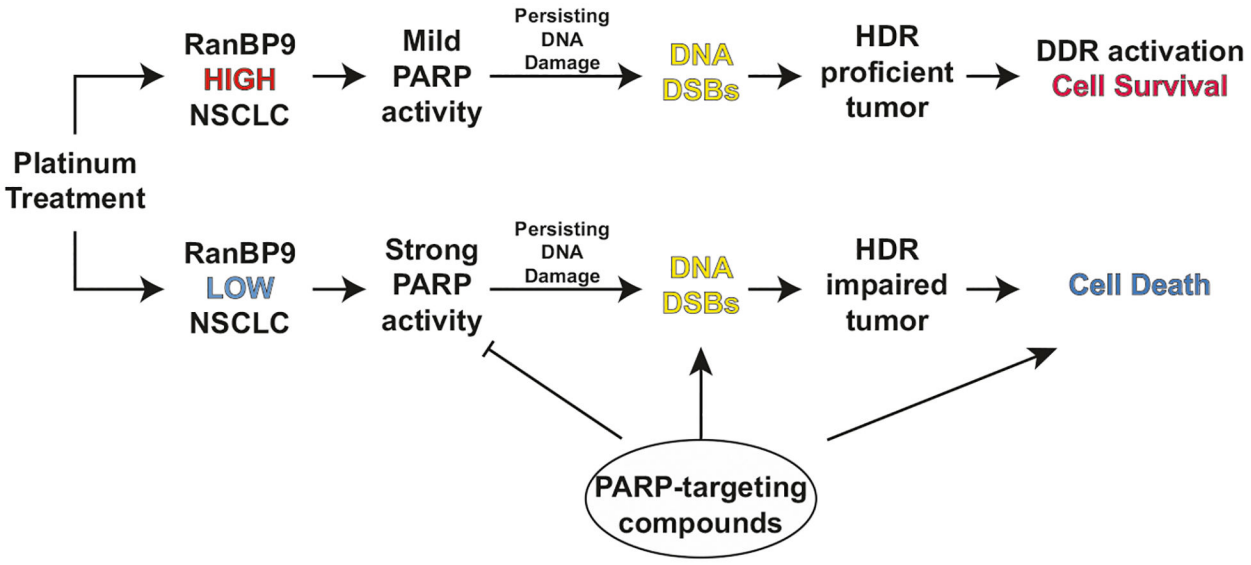

Fig. 7.

RANBP9 levels in NSCLC as a potential biomarker of response to DDR-targeting therapies. In RANBP9 positive NSCLC tumors, the cellular response to persisting DNA-damaging agents mostly relies on a proficient ATM-HDR axis: the activation of DNA repair (DDR) results in cancer cell survival and resistance to genotoxic stress. Conversely, RANBP9-low or -negative tumors display a defective HDR and activate different repair mechanisms, such as PARP-dependent DNA repair, to cope with DNA-damaging agents. However, DNA DSBs can be induced by persisting genotoxic stress and enhanced by co-treatment with PARP-targeting compounds to prevent PARP-mediated repair. The simultaneous inhibition of the PARP-dependent repair and the absence of efficient HDR-repair result in cancer cell death